Available online at www.sciencedirect.com
ScienceDirect
Journal of the European Ceramic Society 30 (2010) 2577–2583
www.elsevier.com/locate/jeurceramsoc

Effect of microstructure on lifetime performance of barium titanate ceramics under DC electric field loading

Yin-Hua Chen, Wei-Hsing Tuan *, Jay Shieh

Department of Materials Science & Engineering, National Taiwan University, Taipei 106, Taiwan

Received 30 January 2010; received in revised form 6 May 2010; accepted 18 May 2010
Available online 12 June 2010

Abstract

Bulk barium titanate ($BaTiO_3$) ceramic specimens with various amounts of abnormal grains are prepared. A direct current (DC) electric field of 6 MV m^{-1} is applied to the specimens and their lifetimes are evaluated. Comparing to the specimens with only small normal grains, the time to failure of the specimens with coarse abnormal grains is significantly shorter. It is found that the $BaTiO_3$ specimens would fail within 200 h when abnormal grains are present in the microstructure. However, the lifetimes of the specimens containing abnormal grains vary significantly from one to another. The Weibull statistics is adopted to estimate the extent of data scatter. The statistical analysis indicates that the amount of abnormal grains has little influence on the lifetime performance of bulk $BaTiO_3$ ceramics under large DC electric fields. In most of the failed $BaTiO_3$ specimens, regardless of their lifetimes, large through-thickness round holes with recrystallization features are present. A mixed failure mode consisting of avalanche and thermal breakdowns is observed for the failed specimens.

Keywords: $BaTiO_3$; Microstructure-final; DC electric field; Dielectric breakdown

1. Introduction

With relatively high dielectric constants, barium titanate ($BaTiO_3$)-based oxides have been widely adopted as the dielectric materials for ceramic capacitors.[1] The application of $BaTiO_3$ thin films as the tunnel barriers for ferroelectric random access memories (FERAMs) has also been proposed recently.[2] Due to the increasing demand on device miniaturization, the required thickness of the dielectric layers in electronic components is continuously decreasing. For example, the dielectric layer thickness in multilayer ceramic capacitors (MLCCs) has now been reduced down to 1 μm and the typical tunnel barrier thickness in FERAMs is as small as 2–3 nm.[2,3] One of the biggest effects from the ongoing trend of device miniaturization is the increase in electric field strength experienced by the dielectric layer, resulting in its premature failure. A considerable literature currently exists concerning the reliability and fatigue behaviors of ferroelectric ceramics under alternating current (AC) electric fields.[4–12] Additionally, a recent study by the authors shows that the lifetime performance of $BaTiO_3$ ceramics under AC electric fields depends strongly on the amount of coarse abnormal grains present within the microstructure.[13] In contrast, the effect of material makeup, such as the microstructure, on the failure behaviors of ferroelectric ceramics under high direct current (DC) electric fields has received little attention. This insufficiency shall be addressed in the present study. Considering nowadays that most portable electronic and communication devices are operated under DC voltage, the reliability of the dielectric layers within the devices under sufficiently large DC electric fields is becoming an important issue.

The microstructure of $BaTiO_3$ is sensitive to its composition, especially to the Ba/Ti ratio and the amount of impurity.[14] A slightly lower than 1, Ba/Ti ratio will induce the formation of a liquid phase above the eutectic temperature (1312 °C) of $BaTiO_3$–$Ba_6Ti_{17}O_{40}$.[14,15] The presence of the liquid phase could trigger the growth of abnormal grains during sintering. A bimodal grain size distribution is thus commonly observed in the Ti-rich $BaTiO_3$ specimens. Internal stresses within the microstructure are commonly induced when cooling through the Curie temperature. Depending on the grain size, the resultant residual stresses could initiate spontaneous cracking.[16] Based on thermal expansion analyses, the presence of abnormal grains

* Corresponding author. Tel.: +886 2 33663899; fax: +886 2 23659800.
E-mail address: tuan@ntu.edu.tw (W.-H. Tuan).

0955-2219/$ – see front matter © 2010 Elsevier Ltd. All rights reserved.
doi:10.1016/j.jeurceramsoc.2010.05.015

within the sintered bulk $BaTiO_3$ ceramics has been related to the formation of microstructural defects and microcracks.[17] Considering the complexity of the grain growth behavior in $BaTiO_3$ and its importance as a dielectric material within commercial electronic devices, an examination of the relationship between the microstructural features of $BaTiO_3$ and its reliability under DC electric field loading is indeed necessary.

There are two major types of lifetime failures in the dielectric materials: (1) dielectric breakdown that takes place at low temperatures under a very high electric field and (2) resistance degradation at elevated temperatures caused by the electromigrations of oxygen vacancies and the resultant electron-hole pairs. For this particular study, the former type of failure (i.e., dielectric breakdown) is of interest. In the present study, bulk $BaTiO_3$ ceramic specimens with various amounts of abnormal grains are prepared and their failure time under high DC electric fields at room temperature are determined. The failure criteria for the specimens are decided based on standards commonly adopted in highly accelerated life tests (HALT), which are frequently employed to examine the reliability of dielectric materials.[18,19]

2. Experimental procedure

A commercial $BaTiO_3$ powder (NEB, Ferro Co., USA) with a reported Ba/Ti ratio of 1.000 ± 0.002 was used as the raw material. The powder was ball-milled in ethanol with zirconia balls for 4 h, followed by drying at 100 °C for 24 h. The resulting powder mix was sieved (150 mesh) and pressed into sample discs of diameter 10 mm at 30 MPa. The discs were then pre-heated at 600 °C for 1 h with both the heating and cooling rates of 1 °C/min to remove any organic residues. After pre-heating, the sample discs were sintered at 1320–1410 °C for various dwell times (5 min to 2 h) in a covered alumina crucible with both the heating and cooling rates of 5 °C/min. Notice that different sintering parameters were designed to produce $BaTiO_3$ specimens of different microstructural features.

Crystalline phases of the sintered $BaTiO_3$ specimens were confirmed using X-ray diffractometry (XRD; MXP18, MAC Science Co., USA) with Cu $K\alpha$ radiation. Densities of the sintered specimens were determined by the Archimedes' method. Polishing and etching steps were carried out on the specimens for the observation of microstructures. Surfaces of the specimens were ground with SiC papers and polished with alumina slurry. The microstructural features at the polished surfaces were revealed by thermal etching at temperatures 100–150 °C below the sintering temperatures and then examined using scanning electron microscopy (SEM; XL30, Philips Co., The Netherlands). The sizes of the grains were verified by sketching the grain boundaries from the SEM micrographs, and the area of each grain was determined by an image analysis technique.[20] By assuming each grain had a spherical shape, the grain diameter could be approximated from the grain area. In order to estimate the grain size distribution for each sintering condition, more than 800 normal and/or 600 abnormal grains were counted.

DC electric field loading experiments on the sintered $BaTiO_3$ specimens were carried out in a silicon oil bath at room temperature. Periodic checks were made on the specimen and oil temperature using remote infrared sensing; it was found that the oil temperature in the vicinity of the specimen remained stable and close to the laboratory (room) temperature throughout the tests. The applied static electric field was in the thickness direction of the specimens and of magnitude 6 MV m^{-1} unless otherwise stated. Silver-based pastes were fired onto the circular faces of the specimens to form the top and bottom electrodes. The diameter of the circular electrodes was 6 mm and the thickness of the specimens was about 500 μm. The electrical loading was supplied by a high voltage amplifier (GPT-615, Gwinstek Co., Taiwan). The DC loading experiments were terminated when the insulation resistivity of the specimens decreased to below 10^6 Ω-cm (i.e., considered failed) or when the loading time exceeded 720,000 s (200 h). The dielectric properties and elastic moduli of the specimens before and after the loading experiments were determined by a LCR meter (2330A, NF Electronic Instrument, Japan) operated at 1 kHz and the ultrasonic technique, respectively. The surfaces and cross-sections of the failed $BaTiO_3$ specimens were examined under SEM.

3. Measurements

The XRD analyses indicate a single phase perovskite structure for all sintered $BaTiO_3$ specimens. Fig. 1 shows the typical micrographs of the $BaTiO_3$ specimens prepared under different sintering conditions. The microstructural properties of the specimens are listed in Table 1. Fig. 1a shows that there are no abnormal grains present in the specimen sintered at 1320 °C for 5 min. When the sintering dwell time is lengthened to 2 h, apart from an increase in density, abnormal grains start to appear in the microstructure with a volume fraction of about 0.38 (see Fig. 1b). A mixture of normal and abnormal grains is also evident in the microstructure of the specimen sintered at 1360 °C for 2 h, within the abnormal grains have a volume fraction of about 0.80 (see Fig. 1c). In contrast, for the specimen sintered at 1410 °C for 2 h, only coarse abnormal grains are observed in the microstructure (see Fig. 1d). The grain size distribution curves for the prepared $BaTiO_3$ specimens are shown in Fig. 2. A bimodal grain size distribution is clearly evident for the specimens sintered at 1320 °C for 2 h and 1360 °C for 2 h. The size variation of the coarse abnormal grains (i.e., the right-hand side peak of the size distribution curve) is substantial. Take the specimen sintered at 1410 °C for 2 h as an example, the size of the coarse abnormal grains varies from 60 to 600 μm. Dielectric measurements listed in Table 1 indicate that the dielectric constant and dissipation factor of the sintered $BaTiO_3$ specimens exhibit a strong dependence on the amount of coarse abnormal grains and the specimen density, respectively. The dielectric constant decreases with increasing amount of abnormal grains, while the specimen density is a good indication of the level of porosity in the microstructure.

The time to failure of the $BaTiO_3$ specimen sintered at 1320 °C for 5 min and loaded under various DC electric field strengths is shown in Table 2. When the applied DC electric field

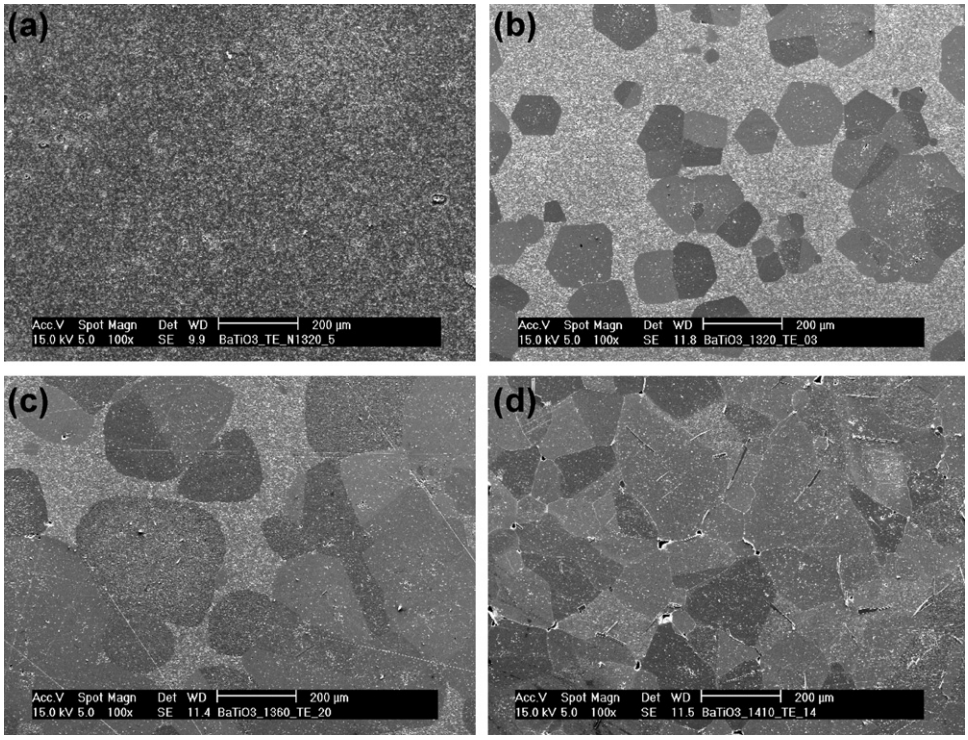

Fig. 1. SEM micrographs of $BaTiO_3$ specimens sintered at (a) 1320 °C for 5 min, (b) 1320 °C for 2 h, (c) 1360 °C for 2 h and (d) 1410 °C for 2 h.

Table 1
Microstructural and dielectric properties of sintered $BaTiO_3$ specimens.

Sintering condition	Relative density (%)	Volume fraction of abnormal grains (%)	Dielectric constant[a]	Dissipation factor[a]
1320 °C/5 min	95.5 ± 0.6	0	3850	0.029
1320 °C/2 h	99.2 ± 0.9	38 ± 7	3380	0.017
1360 °C/2 h	99.2 ± 0.6	80 ± 7	1640	0.019
1410 °C/2 h	97.9 ± 1.0	100	1810	0.021

[a] Average value.

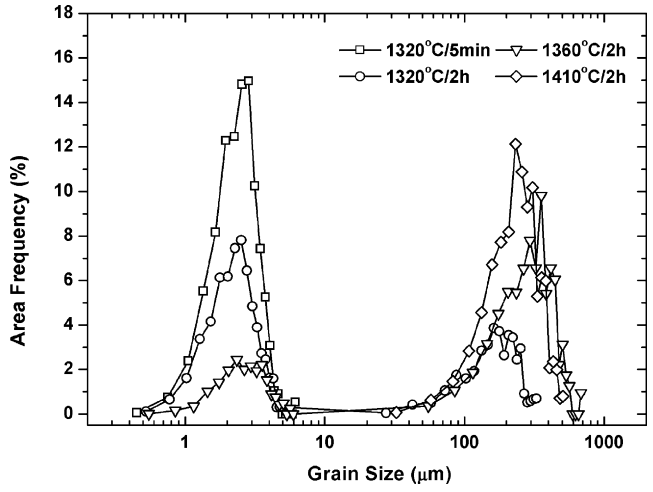

Fig. 2. Grain size distribution curves for $BaTiO_3$ specimens sintered at various conditions.

is set at 6 or 7 MV m^{-1}, no dielectric breakdown is observed within 400 h. Failure of the specimen (i.e., insulation resistivity < 10^6 Ω-cm) occurs only when the electric field exceeds 7 MV m^{-1}. The ratio of the lifetimes under two different applied electric fields can be estimated by the HALT relationship[21]:

$$\frac{t_1}{t_2} = \left(\frac{V_2}{V_1}\right)^n \times \exp\left[\frac{E_S}{k}\left(\frac{1}{T_1} - \frac{1}{T_2}\right)\right] \quad (1)$$

where t is the time to failure (i.e., lifetime), E_S is the pseudo activation energy, V is the DC voltage/electric field, n is the exponent of voltage acceleration, k is the Boltzmann constant, T is the working temperature, and subscripts 1 and 2 represent two different sets of conditions. A value of 3 is frequently adopted for n.[21] From Eq. (1), the lifetime of the $BaTiO_3$ specimen sintered at 1320 °C for 5 min and loaded under 3.6 V μm^{-1} (notice that 3.6 V is the output voltage of a conventional Li-ion rechargeable battery) is estimated to be longer than 3000 h.

The lifetime of the $BaTiO_3$ specimen at a DC electric field of 6 MV m^{-1} is drastically reduced when coarse abnormal grains are formed in the microstructure. The time to failure of the $BaTiO_3$ specimens with different volume fractions of abnor-

Table 2
Time to failure for $BaTiO_3$ specimens sintered at 1320 °C for 5 min (containing no abnormal grains) and loaded under various electric field strengths.

DC electric field strength (MV m^{-1})	6	7	8	9
Time to failure	>500 h	>400 h	~5000–6000 s	~200–300 s

Table 3
Lifetime performance of $BaTiO_3$ specimens containing abnormal grains when loaded at a DC electric field of 6 MV m^{-1}.

Sintering condition	Total # of specimens	# with lifetime <1 s	# with lifetime >200 h	Time to failure[a] (s)	Weibull modulus
1320 °C/2 h	25	2	1	33,849 (1–720,000)	0.41
1360 °C/2 h	30	3	0	39,057 (1–413,308)	0.35
1410 °C/2 h	30	10	0	849 (1–4304)	0.34

[a] Average value.

mal grains is shown in Table 3. For each sintering condition, 25–30 specimens were tested and the measured lifetime values scatter in a wide range. Among the 25 specimens which contain 38% abnormal grains (i.e., sintered at 1320 °C for 2 h), only one survived the loading strength of 6 MV m^{-1} for more than 200 h. All the rest failed within 200 h, including two specimens that failed immediately at the onset of electric field exertion (less than 1 s). The lifetime data listed in Table 3 indicate that as the amount of abnormal grains is increased, the number of specimens with a lifetime less than 1 s is increased. Nevertheless, there is no clear correlation between the average time to failure and the sintering temperature (i.e., the amount of abnormal grains). Furthermore, for the values of time to failure, the data variation is very large. This suggests that even with the same sintering and loading conditions, the lifetimes of the $BaTiO_3$ specimens containing abnormal grains vary significantly from one to another. Fig. 3 shows the distributions of failure time for the $BaTiO_3$ specimens containing abnormal grains. A large data scatter is evident.

In order to evaluate the extent of data scatter, the Weibull statistical analysis is adopted. The Weibull statistics is suitable when the specimen failure is initiated from the structural weak point.[22] To be demonstrated later, the dielectric breakdown in the $BaTiO_3$ specimens is strongly associated with the flaws in the microstructure. The Weibull two-parameter statistics used to quantify the data scatter is given as[22]:

$$\ln\left[\ln\left(\frac{1}{1-F}\right)\right] = m\ \ln\ t - m\ \ln\ t_0 + c \tag{2}$$

where t is the lifetime, t_0 is the characteristic lifetime which corresponds to the 63.2% probability of failure, m is the Weibull modulus representing the extent of scatter, and F is the probability of failure calculated using the following equation:

$$F = \frac{n - 0.5}{N} \tag{3}$$

where n is the nth specimen (specimens are numbered) and N is the total number of specimens in the batch. A smaller m value corresponds to a larger data scatter. The Weibull distributions for the $BaTiO_3$ specimens containing coarse abnormal grains are shown in Fig. 4. The Weibull moduli m derived from the distribution curves vary in a small range from 0.35 to 0.41 (see Table 3). The extent of data scatter is large based on the small moduli.

The circular surfaces of the failed $BaTiO_3$ specimens are examined upon removing the silver electrodes. A typical top surface (where positive voltage applied) micrograph of the failed $BaTiO_3$ specimens is shown in Fig. 5a. A round hole with a diam-

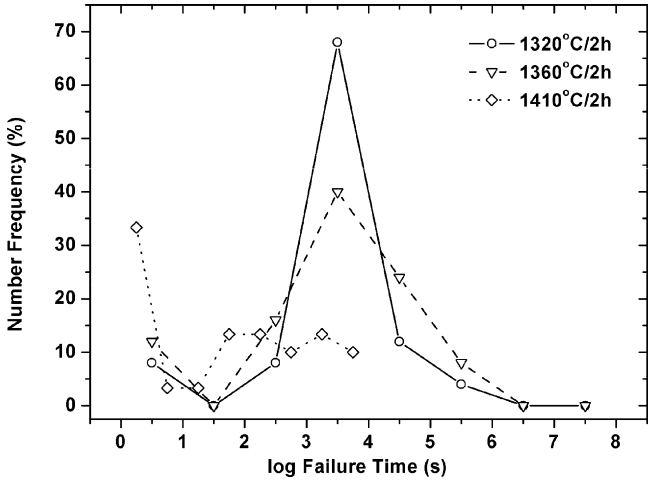

Fig. 3. Distributions of failure time under a DC electric field of 6 MV m^{-1} for $BaTiO_3$ specimens containing abnormal grains.

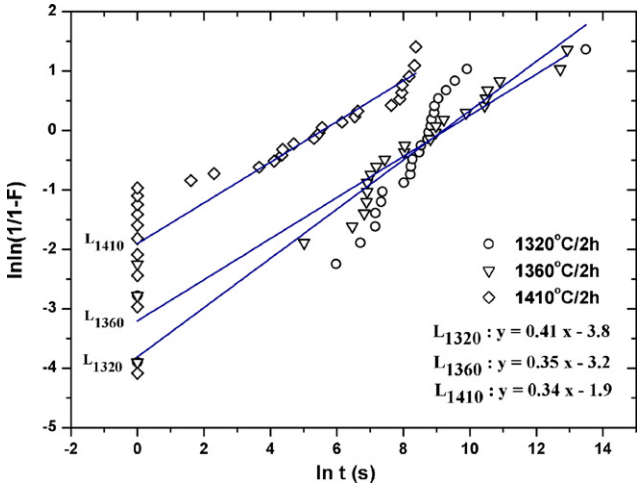

Fig. 4. Weibull distributions for $BaTiO_3$ specimens containing abnormal grains.

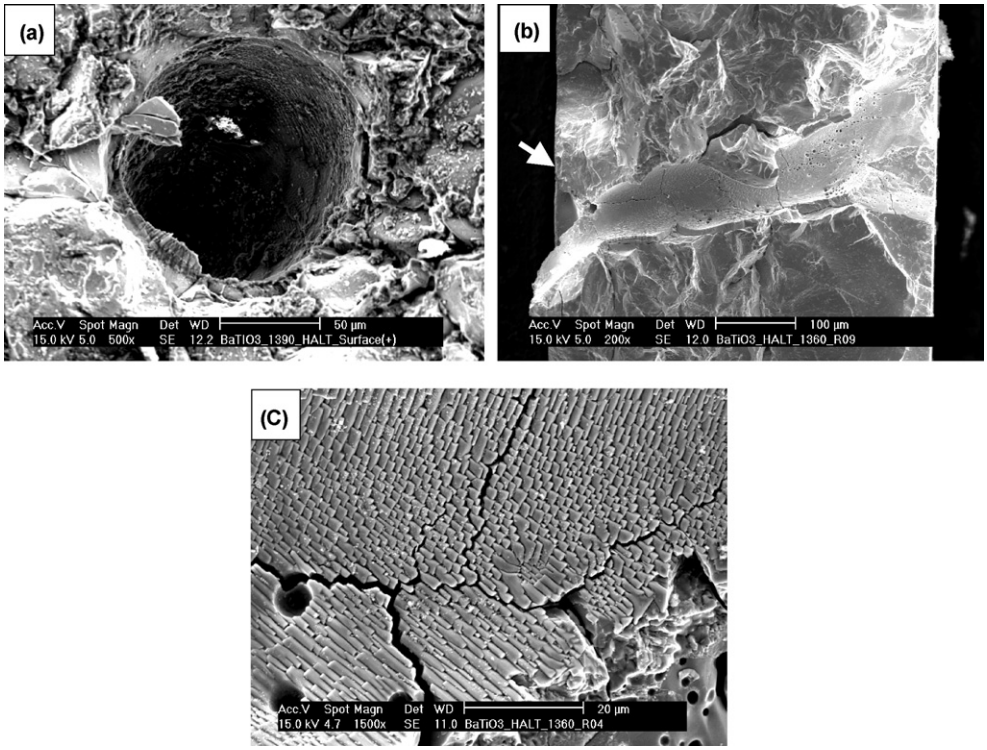

Fig. 5. SEM micrographs of (a) top surface, (b) cross-sectional surface and (c) interior microstructure of the through-thickness round hole in failed $BaTiO_3$ specimens under DC electric field loading. Arrow shown in (b) indicates the top surface.

eter of about 50 μm is observed. The round hole is believed to be caused by the dielectric breakdown and can be observed on the surfaces of more than 90% of the failed $BaTiO_3$ specimens. The cross-sectional micrograph of the hole is shown in Fig. 5b. The hole is through-thickness and runs in a direction approximately parallel to the direction of the applied DC electric field. Fig. 5c shows the interior microstructural features of the hole. It is evident that recrystallization occurs inside the round hole, indicating that the hole is generated by electrical arcing, accompanied by a rapid increase in temperature. Arcing would occur if a sufficiently high electric field leads to thermal runaway of electron emission sites. While a rapid increase in temperature would induce localized melting (and then recrystallization) in the microstructure. This notion is explained further in the next section.

4. Discussion

Two main dielectric breakdown mechanisms for capacitor materials have been suggested in the literature; they are avalanche breakdown and thermal runaway.[21,23,24] Avalanche breakdown is caused by an abrupt rise in current and can be associated with the extrinsic defects (e.g., cracks and pores) of the material. Thermal runaway on the other hand is caused by a gradual increase in leakage current due to temperature rise and can be related to the intrinsic defects (e.g., grain boundary and second phases) of the material. For the $BaTiO_3$ specimens investigated in the present study, a mixed failure mode is observed. The lifetime data indicate that as the amount of abnormal grains is increased, the number of specimens with extremely short lifetimes (<1 s) is increased. This suggests an avalanche-like arcing behavior. However, in most of the failed $BaTiO_3$ specimens, regardless of their lifetimes, the presence of large through-thickness round holes with recrystallization features suggests a substantial increase in temperature at the breakdown site during DC loading, supporting the thermal runaway breakdown mechanism. Based on the experimental evidences, it is believed that avalanche arcing could occur if a sufficiently large DC electric field leads to thermal runaway of electron emission sites, such as the silver electrodes or microstructural defects which contain trapped electrons.

The experimental data show that the lifetime performance of bulk $BaTiO_3$ ceramics under DC electric field loading is strongly influenced by the presence of coarse abnormal grains. The time to failure is significantly reduced with the formation of abnormal grains in the microstructure. Additionally, the large size variation of the abnormal grains leads a large scatter in the lifetime data. The connection between the DC lifetime and the grain features of the $BaTiO_3$ ceramics signifies the importance of microstructural control through material processing. It is evident that the formation of coarse abnormal grains in the $BaTiO_3$ ceramics should be avoided in order to have a quality lifetime under DC electrical loading. The dielectric properties and elastic moduli of the $BaTiO_3$ specimens before and after the DC loading experiments are shown in Table 4. As expected, the dielectric constant and elastic modulus decrease after DC loading, especially for the specimens with a large amount of abnormal grains (i.e., >38%). The decrease in the dielectric constant could be associated with the formation of a current path (i.e., the through-thickness round hole) as demonstrated in Fig. 5. The decrease

Table 4
Dielectric and elastic properties of $BaTiO_3$ specimens containing abnormal grains before and after DC electric field loading at 6 MV m^{-1}.

Sintering condition	Dielectric constant[a]		Dissipation factor[a]		Elastic modulus[a] (GPa)	
	Before	After	Before	After	Before	After
1320 °C/2 h	3380	3040	0.017	2.8	87	85
1360 °C/2 h	1640	300	0.019	12	140	97
1410 °C/2 h	1810	1090	0.021	26	118	94

[a] Average number.

in the elastic modulus on the other hand is likely due to the formation of microcracks.[17] The dissipation factor, which is sensitive to the presence of microstructural defects, increases by 2–3 orders of magnitude after DC loading. Microstructural defects generated during DC loading are joined together and form interconnected channels allowing the leakage current to flow. The buildup of the leakage current results in an increase in temperature which encourages the further rise of leakage current (i.e., a classic thermal runaway scenario). Hence, a significant amount of heat is quickly built up at the potential breakdown site causing localized melting in the microstructure. With the combination of avalanche arcing due to the rapid increase in the leakage current and localized melting due to the heat accumulated, large through-thickness round holes with recrystallization features are formed in the failed $BaTiO_3$ specimens.

The lifetime data of 25–30 $BaTiO_3$ specimens for each sintering condition were used for the Weibull statistical analysis. The confidence level for the calculated Weibull modulus depends strongly on the number of specimens adopted. For a Weibull modulus value of 0.4, the margin of error at a 90% confidence level is ±0.09 when 30 specimens are used.[25] In the present study, the Weibull moduli of the $BaTiO_3$ specimens containing coarse abnormal grains vary in a small range from 0.34 to 0.41. The difference between the moduli falls within the tolerance of a 90% confidence level, indicating a similar reliability for the specimens containing abnormal grains regardless of the sintering condition. Additionally, with the Weibull statistics and the experimental data collected in the present study, the probability of failure for the 500 μm-thick $BaTiO_3$ ceramics under different combinations of applied DC field strength and loading time can be approximated. It should be noted that the probability of failure is critically dependent on the thickness of the ceramic specimen because across different thicknesses, different numbers of grains and grain boundaries are present. In order to predict the probability of failure for the $BaTiO_3$ ceramics of other thicknesses, new sets of time to failure data need to be collected first using specimens of various thicknesses and then fed into the Weibull statistics described in the previous section.

The lifetime performance of the $BaTiO_3$ specimens under DC electric field loading is significantly reduced when coarse abnormal grains are formed in the microstructure. A bimodal grain size distribution is observed for the $BaTiO_3$ specimens sintered at 1320 °C for 2 h and 1360 °C for 2 h; however, the volume fractions of abnormal grains in these two specimens (approximately 38% and 80%, respectively) are rather different. Despite this sizeable difference in the amount of abnormal grains, the experimental data indicates that the average lifetime values and Weibull moduli of failure for the two specimens are very similar (see Table 3). A possible explanation for this is with a volume fraction of either 38% or 80%, the number of coarse abnormal grains is readily sufficient to form a connected network within the microstructure. Since the observed breakdown phenomenon in $BaTiO_3$ is believed to be initiated from the defects associated with the coarse abnormal grains, a connected network of these grains would provide a favorable path for dielectric breakdown. The lifetime behaviors of the $BaTiO_3$ specimens with a bimodal grain size distribution are therefore similar, provided that the amount of abnormal grains is large enough to form a connected network. In contrast, for the specimen containing only coarse abnormal grains (i.e., sintered at 1410 °C for 2 h), a high concentration of microstructural defects would seriously undermine its lifetime performance under DC electric field loading, and as a result, give rise to an average lifetime value much smaller than those of the specimens with a bimodal grain size distribution.

5. Conclusions

In the present study, bulk $BaTiO_3$ ceramic specimens with various amounts of abnormal grains are prepared and their lifetimes under a DC electric field of 6 MV m^{-1} are evaluated. Comparing to the specimens with only small normal grains, the time to failure of the specimens with coarse abnormal grains is significantly shorter. It is found that the $BaTiO_3$ specimens would fail within 200 h when abnormal grains are present in the microstructure. However, the lifetimes of the specimens containing abnormal grains vary significantly from one to another. The extent of data scatter estimated using the Weibull statistics is large. The Weibull moduli derived from the lifetime data of the $BaTiO_3$ specimens with different amounts of abnormal grains vary in a small range from 0.35 to 0.41, indicating a similar reliability. The statistical analysis indicates that the amount of abnormal grains has little influence on the lifetime performance of bulk $BaTiO_3$ ceramics under large DC electric fields. In most of the failed $BaTiO_3$ specimens, regardless of their lifetimes, large through-thickness round holes with recrystallization features are present. A mixed failure mode consisting of avalanche and thermal breakdowns is observed for the failed specimens.

Acknowledgement

Financial support is provided by the National Science Council, Taiwan, under Contract Number NSC98-2221-E-002-057.

References

1. Kishi H, Mizuno Y, Chazono H. Base-metal electrode-multilayer ceramic capacitors: past, present and future perspectives. *Jpn J Appl Phys* 2003;**42**:1–15.
2. Garcia V, Fusil S, Bouzehouane K, Enouz-Vedrenne S, Mathur ND, Barthelemy A, et al. Giant tunnel electroresistance for non-destructive readout of ferroelectric states. *Nature* 2009;**460**:81–4.
3. Pithan C, Hennings D, Waser R. Progress in the synthesis of nanocrystalline $BaTiO_3$ powders for MLCC. *Int J Appl Ceram Technol* 2005;**2**:1–14.
4. Jiang Q, Cao W, Cross LE. Electric fatigue in lead zirconate titanate ceramics. *J Am Ceram Soc* 1994;**7**:211–5.
5. Cao H, Evans AG. Electric-field-induced fatigue crack growth in piezoelectrics. *J Am Ceram Soc* 1994;**77**:1783–6.
6. Shieh J, Huber JE, Fleck NA. Fatigue crack growth in ferroelectrics under electrical loading. *J Eur Ceram Soc* 2006;**26**:95–109.
7. Lynch CS, Chen L, Yang W, Suo Z, McMeeking RM. Crack growth in ferroelectric ceramics driven by cyclic polarization switching. *J Intell Mater Syst Struct* 1995;**6**:191–8.
8. Qian R, Lukasiewicz S, Gao Q. Electrical fatigue response for ferroelectric ceramics under electrical cyclic load. *Solid-State Electron* 2000;**44**:1717–22.
9. Weitzing H, Schneider GA, Steffens J, Hammer M, Hoffmann MJ. Cyclic fatigue due to electric loading in ferroelectric ceramics. *J Eur Ceram Soc* 1999;**19**:1333–7.
10. Nuffer J, Lupascu DC, Rödel J. Damage evolution in ferroelectric PZT induced by bipolar electric cycling. *Acta Mater* 2000;**48**:3783–94.
11. Fang DN, Liu B, Sun CT. Fatigue crack growth in ferroelectric ceramics driven by alternating electric fields. *J Am Ceram Soc* 2004;**87**:840–6.
12. Westram I, Laskewitz B, Lupascu DC, Kamlah M, Rödel J. Electric-field induced crack initiation from a notch in a ferroelectric ceramic. *J Am Ceram Soc* 2007;**90**:2849–54.
13. Lu SC, Chen YH, Tuan WH, Shieh J, Chen CY. Effect of microstructure on dielectric and fatigue strengths of $BaTiO_3$. *J Eur Ceram Soc* 2010;**30**:2569–76.
14. Hennings DFK, Janssen R, Reynen PJL. Control of liquid-phase-enhanced discontinuous grain growth in barium titanate. *J Am Ceram Soc* 1987;**70**:23–7.
15. Rios PR, Yamamoto T, Knodo T, Sakuma T. Abnormal grain growth kinetics of $BaTiO_3$ with an excess TiO_2. *Acta Mater* 1998;**46**:1617–23.
16. Schneider GA, Heyer V. Influence of the electric field on Vickers indentation crack growth in BaTiO3. *J Eur Ceram Soc* 1999;**19**: 1299–306.
17. Tuan WH, Lin SK. The microstructure–mechanical properties relationships of BaTiO3. *Ceram Int* 1999;**25**:35–40.
18. Hobbs GK. *Accelerated reliability engineering: HALT and HASS*. New York: John Wiley & Sons; 2000.
19. Confer R, Canner J, Trostle T, Kurtz S. Use of highly accelerated life test (HALT) to determine reliability of multilayer ceramic capacitors. In: *Proceedings 41st electronic components and technology conference*. 1991. p. 320–2.
20. Chen YH, Lu SC, Tuan WH, Chen CY. Microstructure transition from normal to abnormal grains for $BaTiO_3$. *J Eur Ceram Soc* 2009;**29**: 3243–8.
21. Rawal, B. S. and Chan, N. H., Conduction and failure mechanisms in barium titanate based ceramics under highly accelerated conductions. *AVX corporation product report*, Myrtle Beach, 1984.
22. Weibull W. A statistical distribution function of wide applicability. *J Appl Mech* 1951;**18**:293–8.
23. Kim DK, Um WS, Kim HG. Electric breakdown of the positive temperature coefficient of resistivity barium titanate ceramics. *J Mater Res* 1996;**11**:2002–8.
24. Yang SJ, Kim JW, Ryu DS, Kim MS, Jang JS. Reliability estimation and failure analysis of multilayer ceramic chip capacitors. *Int J Mod Phys B* 2003;**17**:1318–23.
25. Ritter JE, Bandyopadhyay N, Jakus K. Statistical reproducibility of the dynamic and static fatigue experiments. *Am Ceram Soc Bull* 1981;**60**:798–806.